SIMPLIFIED AEROTHERMAL MODELS FOR S/C COMPONENTS (SAM): EXECUTIVE SUMMARY

CR075/15

JULY 2015

J. MERRIFIELD

Fluid Gravity Engineering Ltd
The Old Coach House
1 West Street
Emsworth
PO10 7DX

Tel 01243 389529

E-mail: enquiries@fluidgravity.co.uk

AUTHORISED	J Merrifield
	N Joiner
ISSUE NO	1
DATE	21 July 2015

THIS IS BLANK PAGE

CONTENTS **PAGE NO**

LIST OF FIGURES

LIST OF TABLES

SUMMARY

This document is the executive summary to simplified aerothermal models for spacecraft components (SAM), ESA contract 4000108121. During this project, basic assumptions made for destructive entry analyses were reassessed and, based on the evidence collected, modified where necessary. The recommendation coming from this study can be summarised as:

- The spacecraft trajectory with and without solar panels should be computed in 6DoF
- Spacecraft fragmentation should be rule based rather than occurring at a prescribed altitude
- Updated heating rates should be applied to primitive components based on the audited review performed as part of this study. In general this results in a lower heating rate being applied to components. It is also important to include an assessment on the sensitivity of a heating rate to the landed area and associated casualty risk of debris objects
- Equivalent metal treatments are not appropriate for insulators and ablators, and therefore a more capable thermal response model should be used.

All these recommendation have been implemented into a tool which can be run under the CDF environment to inform early stages of spacecraft design with respect to destructive entry analysis.

Some additional recommendation also came from the present studies which were not implemented directly into the CDF tool, but which have been identified as worthwhile capabilities. The present status of the most important of these developments is given below:

- Tree structure fragmentation based on joints
    - SAM modules have been written to take this into account (fragment tree structure and joint based fragmentation rules) but cannot be activated from the CFD (GUI) tool. An expert user can exercise this capability using a scripted approach.
- Whole spacecraft heating is a difficult problem where the required balance of accuracy, robustness and computational efficiency is still not clear. An increased understanding of the expected accuracy of the panel inclination methodologies in the continuum regime (e.g. the modified Lees approach, the methodology currently used by SCARAB) is needed to define sensible expected accuracy limits for such approaches. This should be the subject of future work.
- Fragmentation phenomenology is still poorly understood. A series of ground tests aimed at identifying the phenomenology, so that it can be properly characterised in further activities, is necessary.
- A Monte-Carlo capability which extends to all the relevant uncertainties and their possible cross correlations needs to be implemented to achieve a sensible understanding of ground casualty risk associated with end-of-life destructive entry. This was identified at proposal stage and needs to be addressed/implemented in future updates of the CDF tool.

1 INTRODUCTION

Thousands of man-made objects are currently in orbit around the Earth. These range from active satellites to flecks of paint, via spent rocket stages and fragments of satellite debris. Due to the drag of the very thin high altitude atmosphere, these objects have slowly decaying orbits, and will eventually re-enter the Earth's thicker, lower atmosphere. Most will be destroyed on entry due to the aerothermal heating experienced at hypersonic velocities at altitudes between 40 and 80km. However, some objects reach the ground.

The processes involved in the re-entry of objects into the Earth's atmosphere are well known. Understanding the phenomena well enough to be able to make predictions about the survivability of particular objects is significantly more challenging. The focus of the present work is on aerothermal predictive methodologies in the context of destructive entry and the impact that simplifications have on the resultant ground casualty risk. For this purpose, an end-to-end software suite (SAM) has been developed to determine the effect of enhancing the aerothermal description of component demise and fragmentation. In particular we investigate: a reassessment of the aeroheating models used for complex and primitive geometries, including tumble averaged and attitude dependant descriptions; thermal response models which account for wall temperature effects, ablation and blowing, and provide an estimate of in-depth conduction to the surface energy balance where deemed significant; extension of ablation mechanisms beyond melting (e.g. for CFRP); rule based spacecraft fragmentation including a treatment of joints; and the significance of 6DoF trajectory propagation both for the spacecraft prior to breakup and for selected fragments. Modelling recommendations are made based on the results of these investigations. In addition, a preliminary identification of knowledge gaps and suggested future developments (e.g. supporting experimental campaigns) is provided.

1.1 Preliminary Down-Selection of Heating Algorithms

This selection was primarily based on correlations already in use at FGE for ~20years:

Primitive	Stagnation	Distribution	Separated flow	Error bars%	Averaging
Sphere	Detra and Hidalgo	Detra and Hidalgo	2% of stagnation	8	Numerical Integration
Plate	N/A	Eckert	2% stagnation	10	Analytic Integration
Cylinder surface	Poll (swept leading edge)	Detra and Hidalgo / Klett	2% stagnation	20	Numerical integration
Cylinder Ends	Klett	Klett	2% of stagnation	20	Numerical integration
Box	As cylinder ends	As Flat plate	2% stagnation	20	Numerical Integration

Table 1 Preliminary Down Selection of Debris Continuum Heating Correlations

2 IMPLIMENTATION AEROTHERMAL ALGORITHMS AND BENCHMARK CASES

A number of aerothermal models have been implemented into the panel code ASPEN [1], which is a component of the SAM code being developed under the present contract. We are primarily concerned with laminar continuum heat flux since this is both a region of high uncertainty and high sensitivity when it comes to the assessment of satellite demise. The models selected for continuum heat fluxes are given in Table 1.

The models described in Table 1 are specific to particular geometries as indicated. Specific models have been implemented for boxes and cylinders along the lines described in the table. As well as these specific

models, generic models (equivalent sphere generalisations) along the lines of the aerothermal model thought to be used in SCARAB (the modified Lees model) are also implemented and assessed.

2.1 Summary of Initial Findings

A range of basic heating algorithms have been implemented into SAM to provide heat fluxes over three dimensional shapes. A basic conclusion is that while equivalent sphere methods (e.g. the modified Lees method used in SCARAB) are fast, easy to code and verify, and are robust, accuracy can be questionable, especially for facetted shapes and trussed frames. Additional high fidelity data (wind tunnel testing or CFD) is required to properly gauge the extent of this. In SAM, an empirical blending is used between stagnation (e.g. Klett) and running length formulations, and this should be updated with high fidelity CFD data or wind tunnel testing. Currently FGE is sponsoring a PhD student at the University of Oxford who is looking at evaluating heat flux distributions over primitive objects at transitional Reynolds numbers using the low density wind tunnel at the Osney Thermo-Fluids Laboratory. These data could eventually be helpful for this calibration process.

Specialist routines which provide a blend between the Klett stagnation formulation and running length correlations are favoured for cylinders and boxes.

3 EVALUATION OF HEATING METHODOLOGIES FOR BASIC TEST CASES

Following on from the initial evaluation of the heating methodologies provided in section 2, we provide a more thorough evaluation of the selected aerothermal models herein. Figure 1 to Figure 6 provides a summary of the performance of the selected SAM models for a cube and compares these data with experimental measurements and higher fidelity (Rtech) CFD results [2]. The shape factor (F_{sh}) is a measure of the heating to a shape averaged over its total surface area. The flux is estimated using an “equivalent” effective spherical radius (R_N). This is shown in equation (3.1)

$$q_{av} = q_s\left(v, \rho, R_N\right) F_{sh} \tag{3.1}$$

where q_s is an analytic expression for stagnation point heating and is a function of free stream velocity and density (v, ρ) as well as equivalent nose radius (R_N). Here q_{av} is the average heating to the shape.

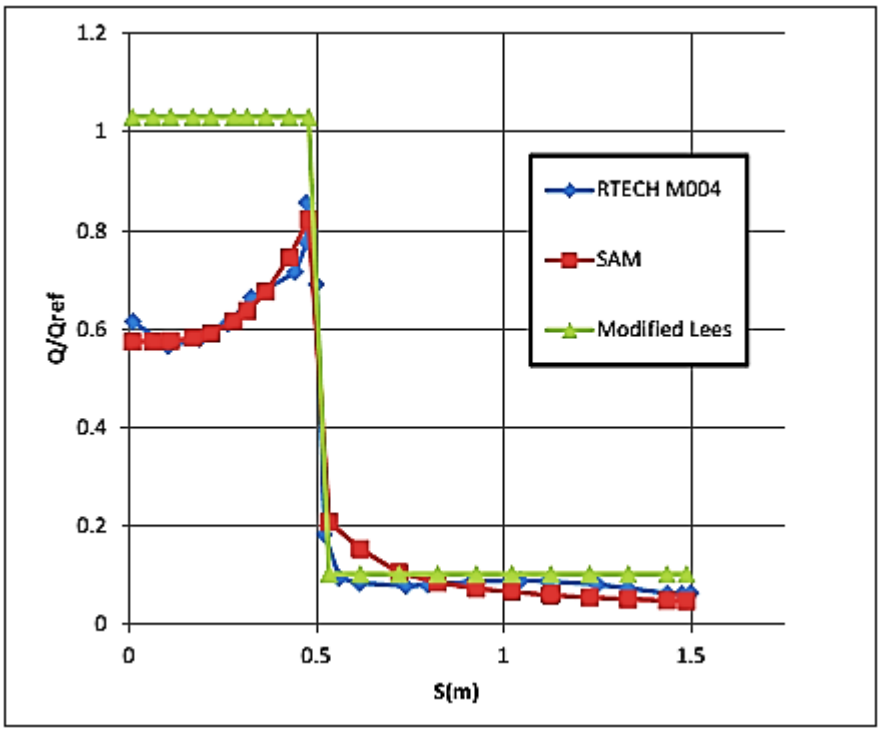

Figure 1 SAM heating test case for end-on cube

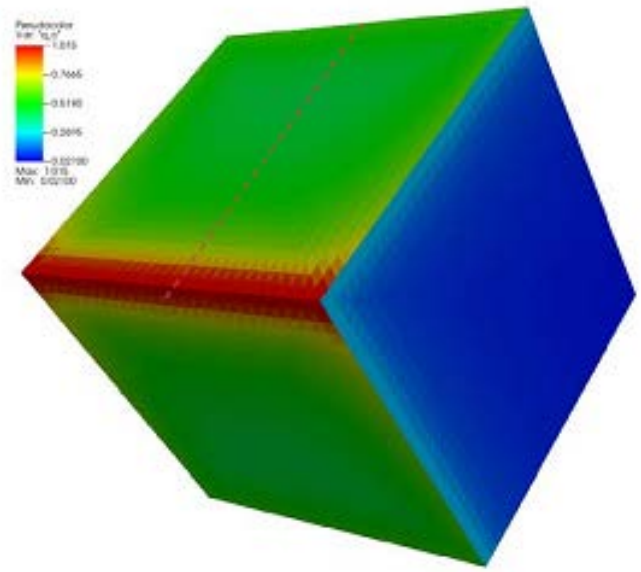

Figure 2 SAM Normalised heatflux for cube at 45 degrees pitch

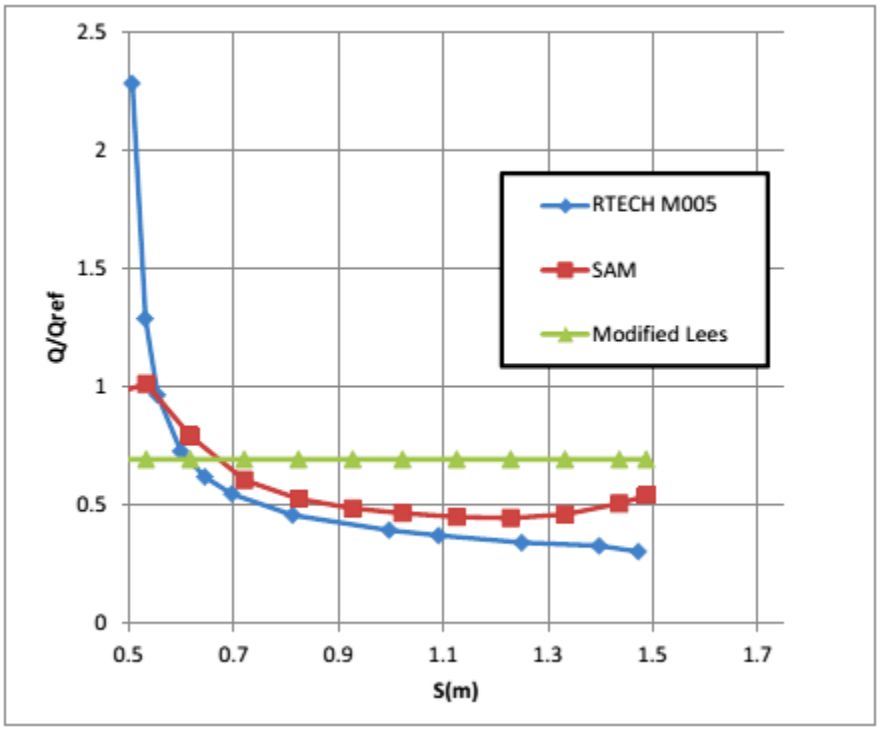

Figure 3 SAM heating test case for 45 degree pitch cube

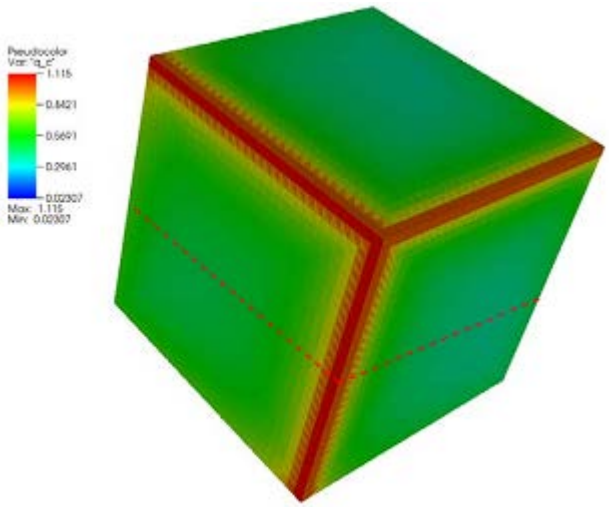

Figure 4 SAM Normalised heatflux for cube at 45 degree pitch and yaw

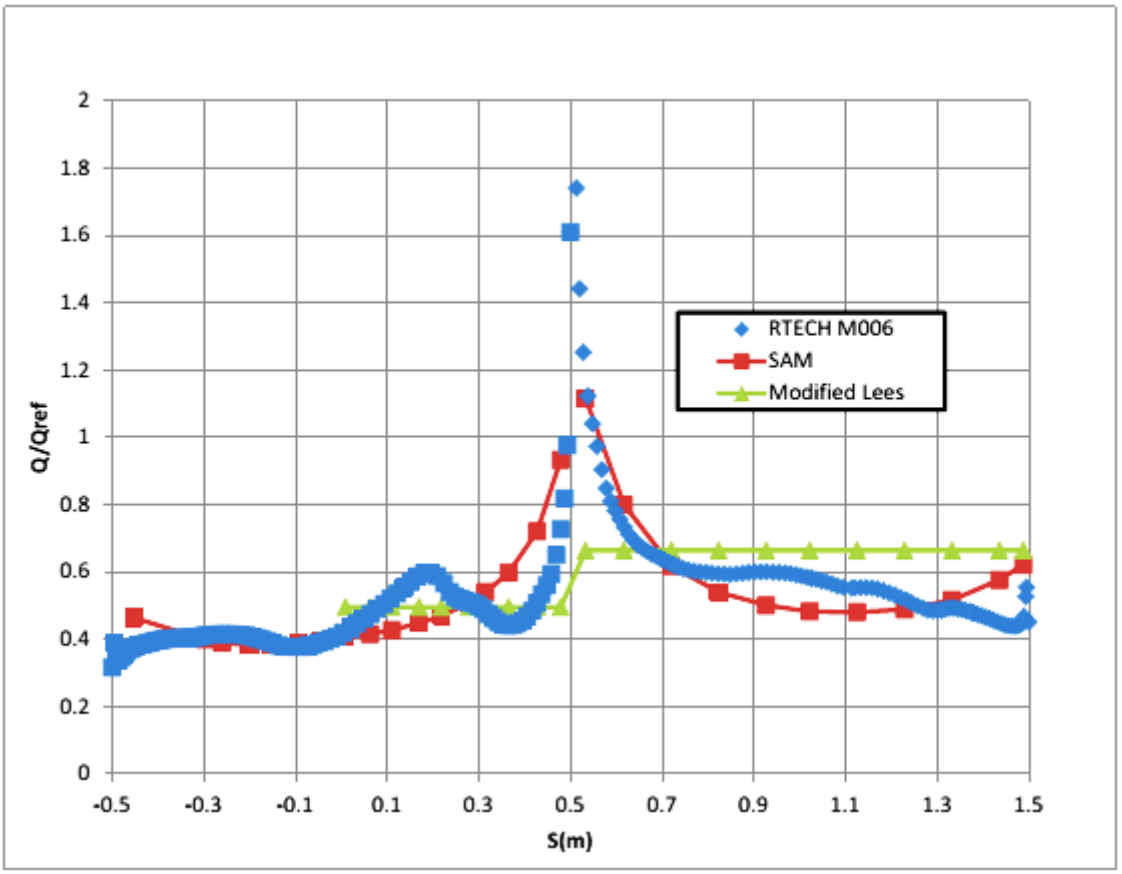

Figure 5 SAM heating test case cube 45° pitch, 45° yaw

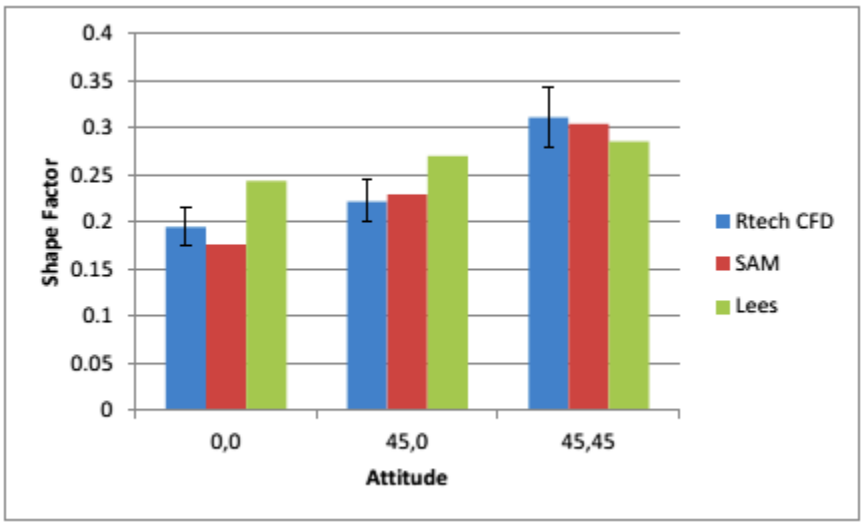

Figure 6 Summary of shape factors for cube test case

A similar comparison for a cylinder is provided in Figure 7 to Figure 9

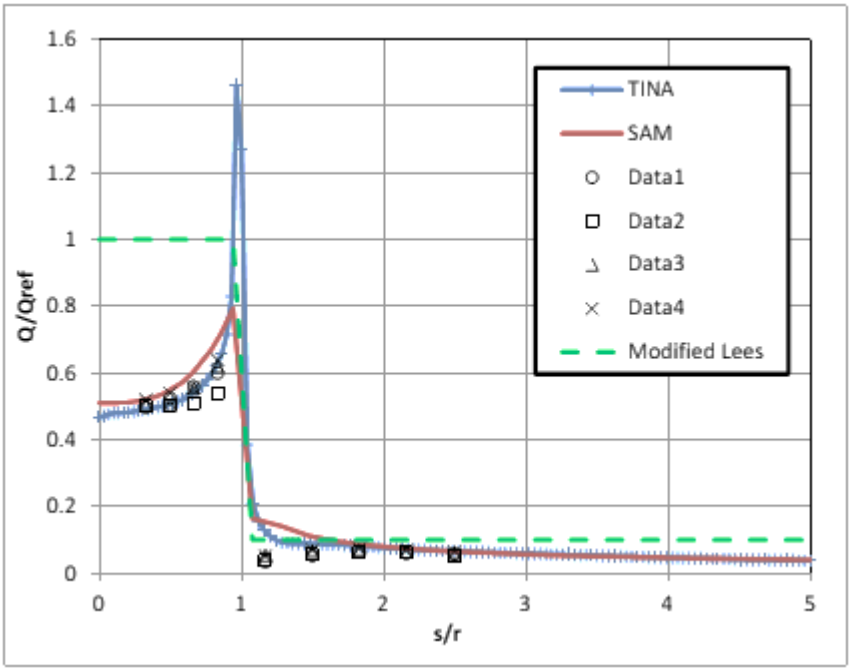

Figure 7 SAM heating test case for end-on cylinder compared with data from Mathews [3]

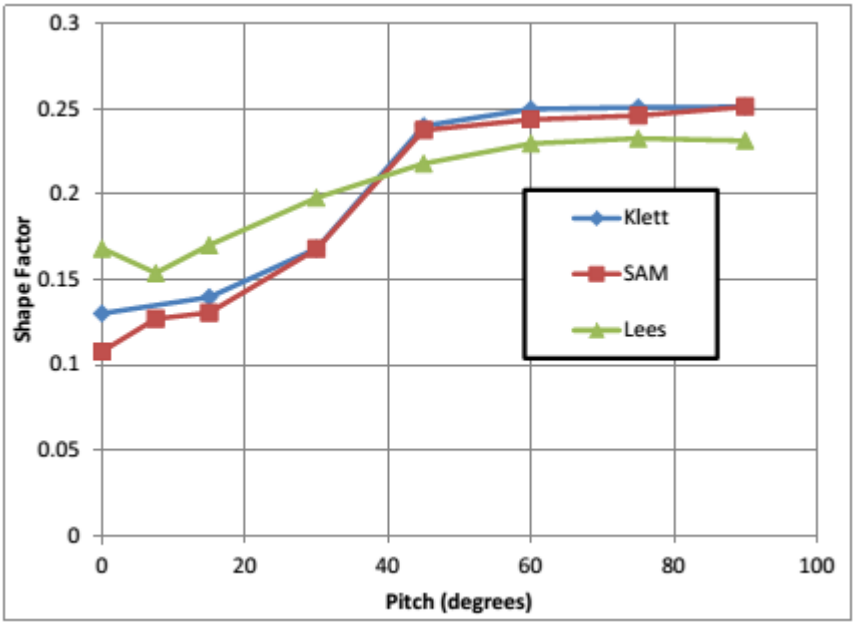

Figure 8 SAM heating test case for cylinder at a variety of pitch angles (Klett comparison [4])

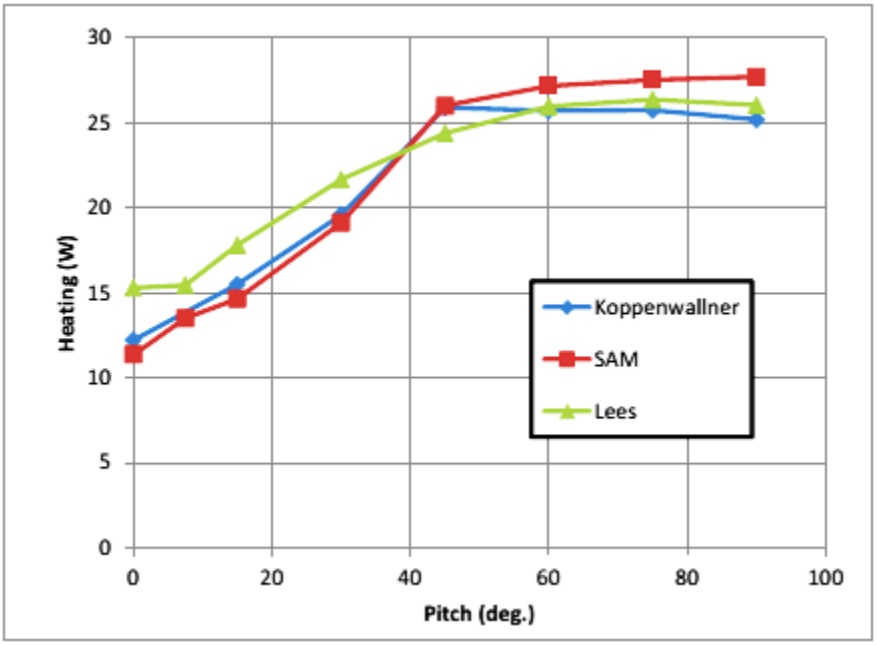

Figure 9 SAM heating test case for cylinder at a variety of pitch angles (transitional) compared with data from Koppenwallner [5]

Figure 9 shows the rarefied-continuum transitional heating (in terms of total power) for a cylinder of *L*/D =2.5. Transitional heating is calculated using the heat flux bridging function of Legge as defined in Ref. [6]

$$St = \frac{St_C}{\sqrt{1+\frac{St_C}{St_{FM}}}} \tag{3.2}$$

Here *St* is the bridged Stanton number and the subscripts *c* and *FM* denote continuum and free-molecular Stanton numbers respectively. For the purposes of the comparison shown in Figure 9, the same free-molecular heating is used for both the SAM and modified Lees methods: only the continuum heating is changed.

4 FRAGMANTATION AND MATERIAL RESPONSE ALGORITHMS

4.1 Literature Review Conclusions

This critical review of the literature has highlighted a number of areas which can be addressed to provide an improved understanding of the fragmentation and demise processes for destructively re-entering spacecraft, as well as an improved estimate of the casualty risk.

The following important observations are made:

- There appears to be little effort to compare and improve models from available flight observation data
- Little effort has been put into understanding of the uncertainties in the process
- Sensitive parameters for survivability and dispersion are suggested, but limited studies on this are reported

- Effort appears to be concentrated on making the models more complex, when the stochastic nature of the process suggests that this is of questionable benefit. It is also unclear that the modelling effort is concentrated on the phenomena which drive the survivability and casualty risk

The following key recommendations are made:

- Significant effort should be made in understanding model performance against flight data – especially from the Hayabusa and ATV-1 events which were well observed
- A comprehensive parametric study on the effects of key parameters should be performed to improve understanding of the drivers of fragment survivability and casualty risk
- Work on understanding the uncertainties in both the modelling and the fragmentation/demise processes is needed
- Modelling effort should be concentrated in the areas where sensitivity is greatest.

Some of this work can be performed within the current activity, but as the focus is on modelling work, much of these recommendations are made in the hope that they are considered in future activities.

The drivers for the uncertainties in survivability and casualty risk are suggested by the literature and the calculations performed by BRL as:

- 6dof Aerodynamics of intact spacecraft (debris footprint driver)
- Upper atmosphere density variation (debris footprint driver)
- Fragmentation altitude (initial fragment heating rate driver)
- Aerothermodynamic heating of fragments (primary goal for activity)
- Emissivity (can drive survivability for high melting point components)

To this end, the following priorities have been identified:

- Provide improved aerodynamics of the intact spacecraft
- Bound the possible fragmentation process altitudes and dispersion effects on the footprint (including explosive effects)
- Account for uncertainties in heating modelling, especially the aerothermodynamic heating and emissivity, to provide uncertainties on survivability
- Heating model uncertainty post processor to feed into casualty risk analysis
- Use of simple internal heating models

It is suggested that this is achieved using a library approach. Higher order methods are employed in order to provide a set of values which can be considered for different spacecraft configurations and debris shapes. Then during runtime, the model can select the appropriate values and uncertainties to be considered within

the aerodynamics, fragmentation and heating modules in order to produce an optimal estimate of the ground casualty risk from a given re-entry scenario.

4.2 Heating and Demise Modelling

An initial verification of the SAM heating and demise models has been performed by comparing the code performance against SESAM (in DRAMA v1.0) and DAS 2.0.2. Being able to match closely the results from both SESAM and DAS has improved the understanding of the modelling within these codes.

A test case is provided with the SESAM module in DRAMA v1.0. This simulation has been run in SESAM and then reproduced using the SAM heating and demise model. The initial conditions are given in Table 2.

Geodetic Latitude	45.2º
Longitude	10.0º
Geodetic Altitude (m)	122000
Speed (m/s)	7300
Bearing	90.0º
Flight Path Angle	-2.0º

Table 2 Demise Test Case Initial Conditions

The parent vehicle is modelled with an augmented drag of 1.43 to account for the solar arrays until 95km altitude. From here the vehicle is modelled without drag augmentation until an altitude of 78km is reached. At this point catastrophic failure is assumed and the separate components are released at an initial temperature of 300K.The components modelled are given in Table 3.

Object	Shape	Width / Diameter (m)	Length (m)	Height (m)	Mass (kg)	Material
Parent	Cylinder	1.7	4.8		1200	
TCU	Box	0.52	0.38	0.27	33	Aluminium
PCU	Box	0.23	0.18	0.16	5	Aluminium
BCDR	Box	0.57	0.31	0.18	19	Aluminium
BCU	Box	0.3	0.2	0.14	4	Aluminium
PPDU	Box	0.41	0.32	0.17	13	Aluminium
Batt	Box	0.54	0.4	0.21	50	Aluminium
Decoder	Box	0.26	0.2	0.19	6	Aluminium
CTU	Box	0.4	0.25	0.25	17	Aluminium
RTU	Box	0.32	0.27	0.25	13.5	Aluminium
MBU	Box	0.24	0.22	0.09	4	Aluminium
TRU	Box	0.2	0.2	0.15	6.7	Aluminium
XPND	Box	0.23	0.17	0.13	5	Aluminium
MTR	Cylinder	0.025	0.74		2.2	Steel
ACC	Box	0.26	0.22	0.13	6.5	Aluminium
MRU	Box	0.29	0.16	0.12	3.5	Aluminium
PDU	Box	0.39	0.3	0.12	11.3	Aluminium
GYRE	Box	0.26	0.2	0.08	3.3	Aluminium
RWL	Cylinder	0.31	0.05		6.1	Steel
RWE	Box	0.22	0.22	0.12	4.5	Aluminium
STRE	Box	0.2	0.16	0.12	3.3	Aluminium
STR	Box	0.2	0.12	0.12	3.0	Aluminium
Tank	Sphere	0.45			5.5	Titanium
Thrsts	Cylinder	0.032	0.13		0.3	Inconel
PL1	Cylinder	0.5	0.66		94	Aluminium
PLE1	Box	0.4	0.25	0.24	15.5	Aluminium
PL2	Box	0.5	0.5	0.5	160	Aluminium
PLE2	Box	0.4	0.25	0.24	18	Aluminium
PL3	Box	0.9	0.4	0.4	45	Aluminium
PLE3	Box	0.25	0.23	0.12	5.3	Aluminium
PL4a	Cylinder	0.17	0.35		13.4	Aluminium
PL4b	Cylinder	0.12	0.22		6.9	Aluminium
PLE3a	Box	0.4	0.25	0.24	18	Aluminium
PLE3b	Box	0.35	0.21	0.19	8	Aluminium
PLE3c	Box	0.32	0.22	0.09	1.9	Aluminium

Table 3 Test Case Objects

In order to reproduce the simulation, the aerodynamics and heating for the separate components are required. These have been inferred from the literature, and a Detra-Kemp-Riddell model for the aerothermodynamic heating is used, consistent with both SESAM and DAS. The parameters used in the SAM representation of the SESAM/DAS simulations are given in Table 4.

	Sphere Radius (R)	Cylinder Diameter (D), Length (L)	Box Sides L,W,H
Reference Area	πR^2	LD	$(LW + LH + HW)/3$
Drag Coefficient Free Molecular	2	$1.62 + 0.73\ (D/L)$	2.55
Drag Coefficient Supersonic	0.92	$0.72 + 0.325\ (D/L)$	1.42
Drag Coefficient Subsonic	0.46	$0.36 + 0.163\ (D/L)$	0.71
Effective Heating Area	$4\pi R^2$	$\pi D(L + D)$	$2(LW + LH + HW)$
Equivalent Nose Radius	R	R	$1.2 * (L + H + W)/6$
Stagnation Point Scale Factor	0.275	$\frac{D}{0.5D + L} * \left(0.161 + 0.043\left(\frac{L}{D}\right)^{0.646} + 0.179\left(\frac{L}{D}\right)\right)$	0.275

Table 4 Aerodynamics and heating of primitives

Comparison of the results from SAM with the SESAM and DAS simulations has revealed two key differences between the SESAM and DAS models. Firstly, the material properties affect the simulation, and secondly SESAM models the effect of the reducing ballistic coefficient on the trajectory where this effect is ignored in DAS.

An initial test of the trajectories can be performed using the Tank titanium sphere object as this does not demise during the entry. Figure 10 demonstrates that the trajectories for the parent object (with and without arrays) and the tank are very similar in SESAM and SAM. Therefore the basic trajectory codes are equivalent and the aerodynamics of cylinders and spheres are sufficiently well represented.

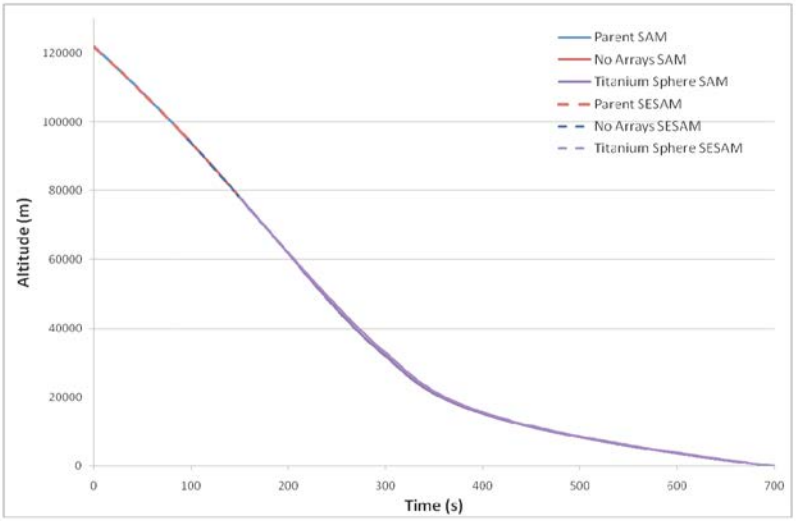

Figure 10 SAM Trajectory Test

This assessment is extended in Figure 11, where three objects are propagated to the ground in SESAM and the equivalent SAM mode. The trajectories are very similar through to 30km altitude, where all the demise is complete in each case.

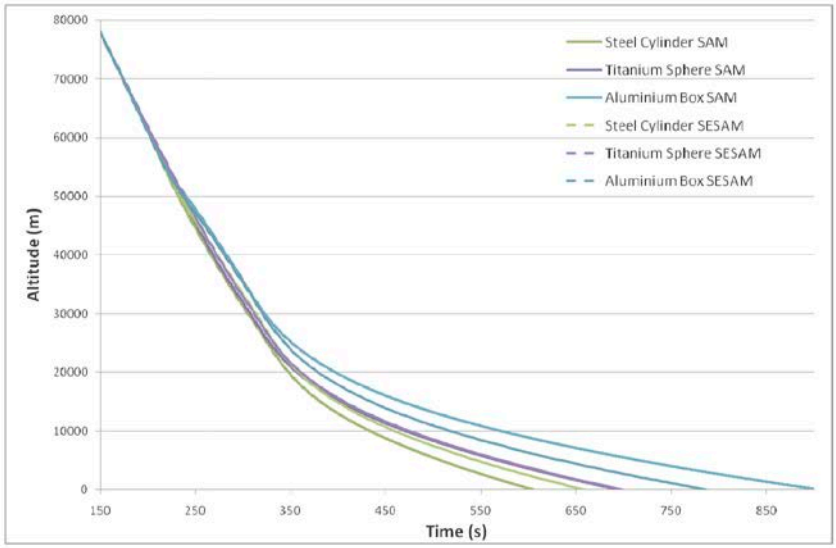

Figure 11 Demise Impact on Trajectory

However, small differences in the heating have an effect on the mass remaining for each object, and thus the ballistic coefficient post-demise is different in SESAM and SAM. This results in the scatter in the trajectories at low altitudes.

The heating differences are assessed in Figure 12, which compares the temperature of the three selected objects in the simulations using SESAM, SAM in SESAM mode, and SAM in DAS mode. The small differences in the heating results in very similar temperature-time curves, but it is worth noting that both the steel cylinder and the aluminium box melt in DAS mode, whereas they survive in SESAM. There are differences in the cooling phase, but these are mainly due to the assumptions of remaining surface area which is smaller in SESAM so the radiative cooling correspondingly lower.

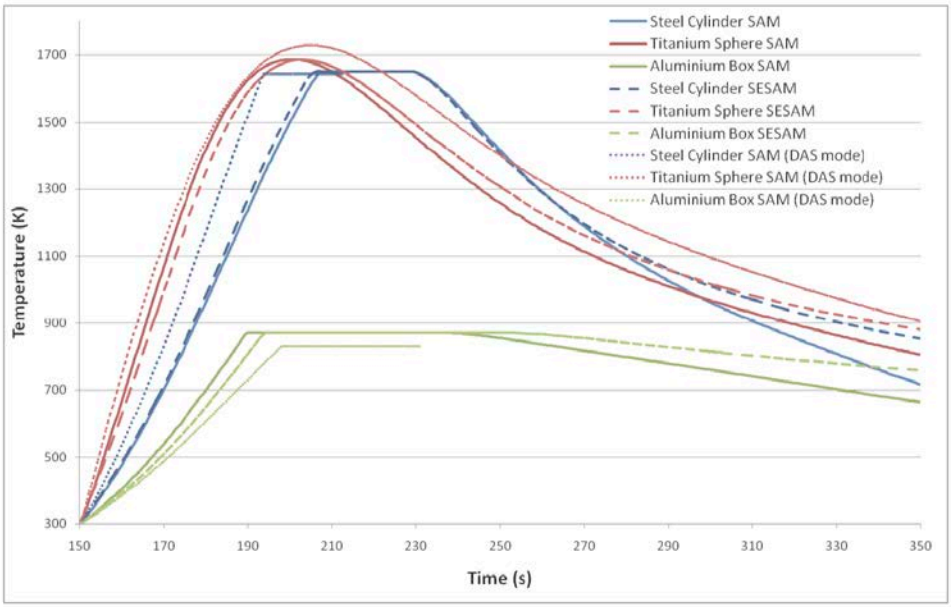

Figure 12 Heating Comparison in SAM (SESAM and DAS modes) and SESAM

This also suggests that object survivability is modelled differently in SESAM and DAS. Table 5 shows the results for each object in SESAM and DAS, and the SAM simulations of each. Where available, the landed mass or the demise altitude is shown. Where an object is predicted to survive the entry, the box is shaded red.

Object	Shape	Demise Altitude/Mass Surviving			
		SESAM	SAM (SESAM mode)	DAS	SAM (DAS mode)
TCU	Box	2.83kg	4.29kg	Survive	48.8km
PCU	Box	63.0km	63.9km	63.8km	64.2km
BCDR	Box	1.09kg	1.21kg	54.1km	55.4km
BCU	Box	66.9km	67.5km	66.2km	68.0km
PPDU	Box	56.8km	0.41kg	55.0km	58.6km
Batt	Box	14.54kg	12.53kg	Survive	Survive
Decoder	Box	63.7km	64.2km	63.0km	64.1km
CTU	Box	0.2kg	0.9kg	56.0km	55.1km
RTU	Box	58.4km	0.46kg	55.4km	57.4km
MBU	Box	64.9km	65.4km	63.1km	64.1km
TRU	Box	60.5km	60.2km	56.3km	59.1km
XPND	Box	61.9km	63.0km	62.6km	61.6km
MTR	Cylinder	62.4km	63.8km	64.3km	65.9km
ACC	Box	60.3km	62.1km	59.6km	60.8km
MRU	Box	65.7km	67.0km	68.1km	68.7km
PDU	Box	58.5km	59.9km	56.9km	59.4km
GYRE	Box	65.8km	66.8km	65.9km	65.5km
RWL	Cylinder	2.4kg	2.7kg	58.8km	58.5km
RWE	Box	63.7km	64.9km	62.0km	63.6km
STRE	Box	64.9km	65.9km	65.5km	64.6km
STR	Box	63.5km	65.5km	66.8km	64.1km
Tank	Sphere	5.5kg	5.5kg	Survive	Survive
Thrsts	Cylinder	68.2km	69.1km	68.2km	70.5km
PL1	Cylinder	29.6kg	36.0kg	Survive	Survive
PLE1	Box	54.3km	0.7kg	57.3km	56.3km
PL2	Box	90kg	98kg	Survive	Survive
PLE2	Box	0.2kg	1.1kg	54.4km	54.0km
PL3	Box	6.2kg	7.0kg	51.5km	50.2km
PLE3	Box	62.7km	64.1km	61.3km	62.8km
PL4a	Cylinder	50.4km	0.62kg	55.0km	50.7km
PL4b	Cylinder	49.7km	53.2km	56.6km	52.6km
PLE3a	Box	0.3kg	1.1kg	54.4km	54.0km
PLE3b	Box	61.4km	62.8km	63.8km	61.7km
PLE3c	Box	71.2km	72.1km	72.3km	70.9km

Table 5 Demise Results

It is clear that the object survivability in DAS is significantly different from that in SESAM. DAS predicts four objects surviving, where SESAM predicts 11. That this is due to the material properties and the ballistic coefficient feedback to the trajectory can be seen from the SAM simulations. In DAS mode, SAM predicts only one object to have a different fate from DAS, and this object demises at very low altitude. However, in SESAM mode, SAM predicts results in line with SESAM. Indeed, the survivability differences are in four objects which land with masses less than 1kg in the SAM model. Use of the shell model can be seen to be slightly conservative in comparison with the area change of the demise model employed by SESAM. The demise altitudes in SAM are in general slightly above those reported by the other codes as the objects are removed at the 15J threshold rather than at complete melt, although the agreement is very good in both modes.

This demonstrates that SAM is capable of replicating results from both the SESAM and SAM codes and that future development, especially in the heating models, can be compared directly to provide the impact this would have on existing tools.

4.3 Fragmentation Modelling

Basic models for the following fragmentation criteria have been investigated in SAM.

- Fixed Altitude Fragmentation
- Fixed Dynamic Pressure Fragmentation
- Fixed Heat Soak
- Fixed Heat Soak multiplied by instantaneous dynamic pressure.

“Physics based” model investigates are:

- Fixed Temperature Fragmentation
- Buckling Failure
- Bending Moment Failure
- Thermal Stress Failure

Basic verification of the fragmentation model has been performed in 6DoF. The box is represented by a cuboid component of 2.5m x 2m x 2.5m, both solar arrays by flat plate components of 3m x 3.8m and the arrays are attached to the box by joints. The joints are at 1.25m from the centre of gravity and are coplanar with the centre of gravity and the solar arrays.

Each of the components and joints has a surface heating point. Tests are performed using the Detra- Kemp-Riddell stagnation point heating with a 0.275 shape factor and an equivalent nose radius of 1.5m on all components for simplicity. The central box is aluminium and the solar arrays have Gallium Arsenide surfaces.

The mass of the vehicle is 1560kg and the principle moments of inertia of 2700kgm^2, 133kgm^3 and 2700kgm^3.

The initial conditions are given in Table 6.

Geodetic Latitude	-38.32º
Longitude	158.49º
Geodetic Altitude (m)	133686
Speed (m/s)	7535
Bearing	129.58º
Flight Path Angle	0.1167º
Initial Orientation	Solar array normal to flow
Initial Rotation Rates	Zero

Table 6 Fragmentation testing initial conditions

Condition	Value	Source
Critical Bending Moment Cold (Nm)	5500	Break at 75Pa consistent with previous experience
Bolt Stress Cold (MPa)	20	High Value for steel bolt from literature
Differential Thermal Expansion (K^{-1})	0.000001	Assume materials selected for similar expansion
Buckling Force (N): Three principal axes	110000 47000 47000	Buckling force as a margin over launch loads: Selected force approximately 7g axial, 3g lateral

Table 7 Nominal fragmentation thresholds for testing

Using reasonable estimates for the cold breaking stresses of the joints and components which are given in Table 7, the first fragmentation event was the bending moment buckling of a solar array joint. This occurred at an altitude of approximately 91km. The sensitivity to changing the orientation, rotation rate and the critical bending moment is given in Table 8.

Test	Failure Altitude (km)
Normal	91.2
45º pitch	91.2
90º pitch	91.2
45º yaw	91.2
90º yaw	91.2
Angular Rates (5,0,0) (deg/s)	91.2
Angular Rates (0,0,5) (deg/s)	91.1
Angular Rates (20,0,0) (deg/s)	91.0
Angular Rates (0,0,20) (deg/s)	91.1
Critical Moment 6000 Nm	90.7
Critical Moment 5000 Nm	91.7

Table 8 Solar Array Bending Moment Failure

Although the time taken to reach the altitude at which the joints fail varies with the initial orientation and the rotation rate of the vehicle, the breaking altitude itself is insensitive. Indeed, the breaking altitude is not highly sensitive to the critical moment; rather the increase in atmospheric density dominates.

Suppressing the bending moment failure allows testing of the other failure modes. Thermal buckling is then seen to occur at 89km with the current values, although the temperature has reached only 580K. Increasing the bolt stress to 25MPa reduces the altitude at which thermal buckling occurs to 82km (temperature 650K), and increasing to 30MPa results in stress buckling occurring first. Clearly, the stresses for bolts/fasteners and the differential thermal expansion coefficients used can vary, but these values are thought to consider low differential thermal expansion and high bolt strength. Varying the heating by ±10% results in a change in the fragmentation altitude from 86.5km to 91.5km.This suggests that this is an important consideration in the fragmentation of a vehicle and should be investigated further.

Suppressing thermal as well as bending moment failure allows assessment of the stress buckling of components. The critical values quoted are reasonably sensible given the manner in which the spacecraft are designed to be as light as possible, but to survive launch loads. This results in stress buckling of the main spacecraft body at 75km, which is broadly in line with observations. This has also been tested with ±10% on the heating and the sensitivity of the fragmentation altitude is found to be less than 1km. It is worth noting that the temperature of the box at this point is 720K, close to the melting point of aluminium. If the strength of the spacecraft is increased by 50%, the stress buckling occurs at 70.5km, still prior to the melting of the component.

If all the fragmentation modes are disabled, the component reaches melt temperature at 62km. Changing the heating by ±10% results in the altitude at which the melt temperature is reached varying from 53km to 67.5km. From these results a table of approximate fragmentation altitudes resulting from the various fragmentation criteria can be constructed for this test case. This is shown in Table 9.

Fragmentation Criterion	Failure Altitude (km)	Sensitivity
Bending moment failure for solar array	91km	VERY LOW
Thermal failure of satellite structure	<75km to 91.5km	HIGH (MEDIUM to heating)
Buckling failure of satellite structure	70km to 75km	MEDIUM
Reach melting point	53km to 67.5km	HIGH

Table 9 Summary of Fragmentation Altitudes in Test Case

All the physics based modes of failure within the SAM fragmentation model have been exercised by this test case, and reasonable results have been obtained, given the approximate nature of the physical data being used. Further, this has allowed a basic investigation into the sensitivity of the fragmentation models to different parameters.

Testing of the demise model shows that comparable results to both SESAM and DAS can be obtained with different options of the SAM code, verifying the basic trajectory, heating and melting models.

4.3.1 Heat Balance Integral Method

4.3.1.1 Literature Survey

The heat balance integral (HBI) technique was developed by Goodman [7] and involves assuming a profile for the temperatures within a material. This reduces the one-dimensional heat conduction equation to a set of Ordinary Differential Equations which can be integrated in time only. An outline of such a scheme and its application to charring ablators is provided by Potts [8], where the equations are integrated using a repeated bisection method at each timestep.

An important restriction of many HBI schemes is that the assumed profile often has a strictly negative temperature gradient at the material surface, and so is only appropriate for the heating phase of a trajectory. A number of schemes are suggested in Potts [8], and a set of profiles which can be used for the heating and cooling phases are suggested by Leone et al. [9]. It is a known problem that the performance of HBI models in the cool-down phase is significantly weaker than that in the heating phase. However, as material demise primarily occurs in the heating phase, errors which might be present in the cooling phase might be considered acceptable.

Both Potts and Leone at al. also include an explicit description of Arrhenius rates in their material charring models which is a complexity beyond that currently envisaged for SAM. Carbon recession is calculated with the use of blowing parameter (B') tables which is also beyond the heat of ablation model used in SAM. This does demonstrate, however, that additional effects can be included to a relatively high fidelity within the HBI framework, and thus the implemented model could be extended in future.

4.3.1.2 Model Selection for SAM

Of the available models in the literature, the required balance between complexity and efficiency for a charring ablator for the SAM code was not to be found. Therefore, some adaptation to the modelling has been performed. The Leone et al. [9] model was selected as a baseline as is has a simple description for both the

heating and cooling phases, but in order to retain the fast engineering code of SAM, a simplified charring model and numerics have been used.

4.3.2 HBI Model Conclusion

Following assessment of the ablation and insulation models in SAM, the heat of ablation model has demonstrated to be sufficiently accurate, but the heating model for insulators can be improved as data already calculated within the SAM model is not fully utilised. A heat balance integral algorithm can be run using this information and is of a suitable fidelity and performance for the SAM application. Currently methods have been adapted to the needs of SAM and such a heat balance integral model has been implemented. This provides a significant improvement in the insulator and ablator modelling within SAM, with a minor impact on runtime. The Mezines correlation has been retained as an option within SAM, but is no longer the default algorithm for standard materials within the SAM library.

5 CONCLUSIONS AND RECOMENDATIONS

During the development of the SAM software, the consequences of aerodynamic and aerothermal simplifications have been investigated and reported in the open literature ([10] [11] [12]), leading to a number of recommendations.

- For object-orientated analysis, conditions at the point of unitary breakup strongly effect fragment survivability. As such, we would recommend performing the trajectory propagation of the spacecraft up until breakup in 6DoF.
- Similarly, breakup altitude is a key driver of fragment survivability and rule based breakup methodologies should replace the prescribed altitude method commonly applied. Some potentially promising rule based techniques have been identified.
- Material properties should be harmonised across the various codes present in the literature to aid code-to-code comparison.
- Insulators and charring ablators are not well represented as equivalent metals and require a different treatment. A HBI methodology has been implemented within SAM to model these materials.
- A review of aeroheating methodologies has generated a revised set of recommended shape factors to be used in object-orientated analyses.
- The limitations of local surface panel inclination techniques have been explored using the modified Lees formulation implemented in SCARAB as an example. Reasonable accuracy can be achieved for average heating rates, but local heating rates, or heat transfer at some attitudes can be inaccurately represented. Panel inclination methods in destructive entry analysis are attractive due to their simplicity and robustness, but a balanced approach in terms of fidelity is needed for calculations that take these heat fluxes as inputs.

Based on the current state of knowledge, the following activities are recommended in order to improve the reliability of destructive entry assessments.

- The knowledge of the spacecraft fragmentation process needs to be improved. Observational campaigns are helping and these could be used to tune empirical fragmentation or physics based fragmentation criteria. Instrumentation such as REBR is invaluable in this respect and the dissemination of data from these types of observational campaigns may well lead to a step change in the understanding of the fragmentation process. There is also a role for aerothermal fragmentation testing in specialist facilities to progress the state of knowledge in this area.
- A European material properties database is required for demise assessments. The collected experimental data should be compatible with the appropriate thermal response model for each material. Here one should move away from equivalent metal approaches for insulating or thermally decomposing (pyrolysing) materials.
- An increased understanding of complex spacecraft components comprising of many different types of material (e.g. batteries) or modern composite materials (e.g. GLARE) is lacking; the demisability of such components requires experimental characterisation.
- Hypersonic heat transfer to primitive shapes is still poorly dealt with in the literature and there is a role for both CFD [2] and experimental campaigns to provide calibration data for rapid engineering level methodologies.
- Calculating heat transfer to complex spacecraft geometries is a difficult problem and the optimal strategy here is still not clear. The most pragmatic approach would be to apply a simple robust technique, with additional steps taken to explore the sensitivity of the risk assessment in terms of a sensible expected error in the heat transfer rate. This would ideally be performed using a Monte-Carlo type approach. In particular, this point should be addressed to aid spacecraft manufacturers in the identification of promising design for demise spacecraft level strategies (e.g. jettison / opening of panels).

6 DISTRIBUTION

ESTEC R Molina

FGE Contract File C647

7 BIBLIOGRAPHY

[1] L.E. Haynes, "FGE Code ASPEN: A Shading Algorithm for Aerodynamics Database Generation," TR054/11 Issue 4, 2012.

[2] RTech. (2015, June) Spacecraft Demise Workshop. [Online]. http://scdw.rtech.fr/

[3] R, K Mathews and R. H Eaves, "Comparison of Theoretical and Experimental Pressure and Heat-transfer distributions on three blunt nosed cylinders in Hypersonic Flow," AEDC, AEDC-TR-67-148, 1967.

[4] R. D. Klett, "Drag Coefficients and Heating Ratios for Right Circular Cylinders in Free-Molecular and Continuum Flow from Mach 10 to 30, SC-RR-64-2141," Sandia National Laboratory, 1965.

[5] G. Koppenwallner, T Lips, and D Alwes, "WIND TUNNEL AERO-HEATING AND MATERIAL DESTRUCTION TESTS FOR IMPROVED DEBRIS RE-ENTRY ANALYSIS," Proc. '5th European Conference on Space Debris' , Darmstadt, 2009.

[6] G Koppenwallner, B Fritsche, T Lips, and H Klinkrad, "SCARAB - A Multi-disciplinary Code for

Destruction Analysis of Space-Craft During Reentry," 5th European Symposium on Aerothermodynamics for Space Vehicles , 2004, p. 281.

[7] T. Goodman, "Application of integral methods to transient nonlinear heat transfer," in Advances in Heat Transfer., 1964.

[8] R. Potts, "Apllication of integrals methods to ablation charring erosion," J. Spacecraft and Rockets, vol. 32, pp. 200-209.

[9] S Leone, R Potts, and Laganelli A., "Enhancements to integral solutions to ablation and charring," J. Spacecraft and Rockets, vol. 32, pp. 210-216, 1995.

[10] J. Merrifield, J. Beck, G. Markelov, and R. Molina, "Simplified Aerothermal Models for Destructive Entry," 8th European Symposium on Aerothermodynamics for Space Vehicles , Lisbon, 2015.

[11] J. Merrifield, J. Beck, G. Markelov, P. Leyland, and R. Molina, "Aerothermal Heating Methodology in the spacecraft aerothermal model (SAM)," 7th IAASS conference , Friedrichshafen, 2014.

[12] J Beck, J. Merrifield, G. Markelov, and R. Molina, "Application of the SAM Destructive re-entry Code to the Spacecraft Demise Thermodynamics and Integration Test Cases," 8th European Symposium on Aerothermodynamics for Space Vehicles , Lisbon, 2015.

[13] L.O. Cropp, "Analytical Methods Used in Predicting the Reentry Ablation of Spherical and Cylindrical Bodies," Sandia Corp, , Albuquerque, New Mexico, SC-RR-65-187 1965, September.